Arabian Journal for Science and Engineering (2022) 47:9005–9018
https://doi.org/10.1007/s13369-021-06485-8

RESEARCH ARTICLE-MECHANICAL ENGINEERING

Computational Fluid Dynamics Analysis of a Thermocline Thermal Storage Unit for Solar Thermal Applications

Senem Şentürk Lüle[1] · **Azin Asaditaheri**[1]

Received: 30 October 2020 / Accepted: 7 December 2021 / Published online: 27 January 2022

Abstract
Solar power is an important instrument to contribute against world energy demand. The intermittency of solar energy is an issue, but it is possible to constrain intermittency either with direct electricity storage for photovoltaic systems or with thermal energy storage for concentrating solar systems. In this study, a single-tank thermocline storage system filled with solid materials was considered. A computational fluid dynamics analysis of a discharge process was simulated. Streamlines and temperature distributions in the tank due to different porosity, filler material sphericity, and fluid type were investigated during discharge process. The simulation results showed that when the fluid has high volumetric heat capacity, the initial energy stored in the tank increases. In addition, if volumetric heat capacity of the fluid is lower than that for the filler material, initial energy stored in the tank is mainly stored in the filler material which is the optimum operation case. Furthermore, for fluids with high volumetric heat capacity, when the porosity of the tank increases, the amount of energy retained in the tank during discharge cycle increases. On the other hand, the situation is reverse if fluid has lower volumetric heat capacity value. Temperature profiles and streamlines of the three hours of discharge showed that for low values of porosity, higher sphericity value prevents mixing of hot and cold fluid and results in better discharge performance. In addition, sectioning of the tank interior with the walls improved tank performance around 30% and diminished the effect of porosity and sphericity.

Keywords Computational fluid dynamics · Energy storage · Solar power · Thermocline

List of Symbols

g	Gravitational acceleration, m s^{-2}
k	Thermal conductivity, W m^{-1} K^{-1}
L	Tank height, m
K	Permeability, m^2
Da	Darcy number
p	Pressure, N m^{-2}
P	Dimensionless pressure
Pr	Prandtl number
Gr	Grashof number
Re	Reynolds number
d_p	Particle diameter, m
T	Temperature, K
U_0	Initial inlet–outlet velocity
u	Velocity components in x direction
v	Velocity components in y direction
U	Dimensionless velocity x-direction
V	Dimensionless velocity y-direction
x	Cartesian coordinate, m
y	Cartesian coordinate, m
X	Dimensionless Cartesian x-direction
Y	Dimensionless Cartesian y-direction

Greek Symbols

α	Thermal diffusivity, $m^2 s^{-1}$
β	Thermal expansion coefficient, K^{-1}
θ	Dimensionless temperature
ρ	Density, kg m^{-3}
μ	Viscosity, kg m^{-1} s^{-1}
τ	Tortuosity
ξ	Porosity
ν	Kinematic viscosity, m^2 s^{-1}

✉ Senem Şentürk Lüle
senturklule@itu.edu.tr

[1] Istanbul Technical University, Energy Institute, 34469 Maslak, Istanbul, Turkey

Subscripts

c	Cold
eff	Effective
f	Fluid
h	Hot
p	Particle

1 Introduction

As the world energy consumption increases, it is vital to develop new generation capacity. When the environmental concerns are taken into consideration, renewable energy attracts more attention than any other means of generating electricity. One of the renewable sources is the sun. There are several ways to harvest solar energy. Photovoltaic systems use panels to convert solar radiation directly to electricity, whereas concentrating solar power systems use mirrors to reflect and focus sunlight on heat collecting component of the system where heat is transferred to a fluid which is used to generate steam to turn the turbine and generator to generate electricity as in thermal or nuclear power plants. Solar power is a strong collaborator of electricity production especially with concentrating solar systems. Concentrating solar systems have various configurations such as parabolic through, parabolic dish, and central tower [1]. Parabolic through type consists of mirrors and receiver tubes that are at the focus line of the mirrors [2]. The parabolic dish type solar system operates by focusing the sunrays on a focal point by directing all sunrays parallel to the axis of the parabola to its center. The receiver is located at the focal point, and the heat machine on the receiver uses Rankine, Stirling or Brayton cycle for power conversion [3]. In central tower plant, the solar beams that hit the heliostats are directed to the central receiver at the top of the tower, which is located in the middle of the system. Therefore, tower can receive all directed sunrays reflected by the heliostat mirrors and produce steam at high pressure and temperature [4].

The electricity from solar power plant is categorized as intermittent due to the fact that solar radiation cannot be continuously available. As a result, fluctuating demand of electricity cannot be met; therefore, solar power plants are considered non-dispatchable. On the other hand, it is possible to constrain intermittency either with direct electricity storage for photovoltaic systems or with thermal energy storage for concentrating systems. In thermal energy storage, some of the heat from the receiver is stored in the storage unit for later use. Since storing thermal energy is cheaper than storing electricity itself, the focus is on development of thermal energy storage systems. Efficient and cost-effective storage is an important tool to increase the share of solar energy in the electricity market. [5] reported that the production of concentrated thermal energy has become a highly attractive integrated energy production system among all the various renewable alternatives because it has a better potential for dispatchability.

For all the systems described above, energy storage can provide dispatchability. Storage unit could be a two-tank or a single-tank thermocline storage. In two-tank system, cold and hot fluids are stored in different tanks. During charging, fluid from cold tank passes through a heat exchanger if system is indirect or through collector field if system is direct to hot tank. During discharging, hot fluid in hot tank moves from hot tank to cold tank after passing through steam generator. On the other hand, in single-tank thermocline storage, the tank is filled with a filler material, which is the main storage medium. During charging, cold fluid moves from the bottom of the tank toward the heat exchanger and returns to the tank from the top as hot fluid and during the discharge cycle, hot fluid moves from the top of the tank toward heat exchanger and returns the tank from the bottom as cold fluid. Since part of fluid in the two-tank storage system is replaced with a filler material which is usually low cost, single-tank thermocline storage offers cost-effective energy storage [6, 7].

1.1 Analytical Studies

The dimensionless hyperbolic governing equations to simulate thermal storage were derived and numerically solved by [6]. It was shown that this model has flexibility to allow different connection designs for the charge/discharge process of the tank. A simplified dual-phase model with unsteady heat transfer feature was developed by [8]. In this study, since the tank considered has multilayer wall, the heat conduction in the composite wall was considered to be two-dimensional, whereas the fluid flow inside the tank was considered to be one-dimensional along the tank axis. The effect of both convective heat transfer from the bed to the wall and molten salt flow rate on the time-dependent thermal response of the tank was analyzed. The simplified model predicted the temperatures of the molten salt, filler material, and walls. The sensitivity analysis performed by [7] showed that the reservoir height, together with the thermo-physical properties of the solid filler material, has the highest effect on reservoir efficiency. HITEC Molten Salt as fluid and quartzite rocks as filler were deployed by [9] to model transfer of heat between two phases by using interstitial heat transfer coefficient to investigate temperature profiles and discharge efficiency of solar thermal systems. It was concluded that efficiency of the discharge improved when Reynolds's number is small and reservoir height is appreciable.

[10] employed the local thermal equilibrium theory in porous media to develop a two-dimensional numerical model to investigate the heat storage and heat release processes of a thermocline tank. The thermocline layer thickness and

the heat storage efficiency were main focus of the analysis. The results, which were compared against experimental data, showed that stable thermocline layers can form during charge/discharge processes and improvements in volumetric heat capacity of filler material together with flow rate can increase the efficiency of storage tank. [11] indicated that the effective heat transfer coefficient with distributed capacitance method can be used to simulate thermal storage. It was shown that effective heat transfer coefficient increased the reliability of the distributed capacitance method.

In their studies, [12] ignored the thermal losses and expressed the heat transfer equation in terms of endless coordinates to simplify the process of solving and obtaining overall results in terms of performance parameters of thermocline in storage tanks. The simulation with the CIEMAT1D1SF model showed that the performance of the thermocouple reservoir strongly depends on the height of the reservoir and the fluid velocity. [13] identified that tank discharge improves by increasing the height of the tank and by reducing the diameter of the inner filler due to increased thermal uniformity and continuous output of molten salt with high thermal quality. To provide an effective tool for tank design, [14] used the governing equations for fluid-free heat transfer for liquid and solid filler materials and generated power saving curves considering four important parameters, i.e., the dimensions of the storage tank, the properties of the liquid, the properties of filler materials, and the operating conditions.

A new single-phase perturbation model involving a series of expansion solution to disruption model was proposed by [15] to investigate the behavior of packed thermocline thermal energy storage tanks. It was shown that it is an improvement over the current models since it more accurately takes the effect of diffusion into account. Thermal performance of thermocline tank against thermocline thickness was invested by [16] with a transient, two-dimensional, axisymmetric, and local thermal non-equilibrium model. It was recommended that in order to increase thermal performance thermocline thickness should be reduced. The study by [15] was taken one step ahead by [17] by extending the algebraic model to handle non-uniform temperature initial conditions. Thermocline storage performance was studied using a numerical model with three phases (fluid, solid, and wall) and one dimension by [18]. The results showed that there is an optimum interstitial fluid velocity for the highest storage performance. Local thermal non-equilibrium model was considered by [19] to investigate the thermocline stability as a function of Re number. It was found that the Re value 1 provides better stability in the axial and radial direction as well as diagonal than other Reynolds numbers.

1.2 Experimental Studies

One of the experimental studies in the literature is about the relation between the porous manifold and the construction and maintenance of thermal stratification in a storage tank by [20]. The results showed that the stratification occurs at Richardson's number below 0.615 and porous manifolds provide stable thermal stratification due to their capability of reducing the shear-induced mixing between fluids with different temperatures. Another experimental study that investigates the thermocline formation in a tank with packed bed of stones as filler material and air at high temperature as heat transfer fluid was performed by [21]. In addition, a numerical and dynamic heat transfer model to calculate thermal properties and physical variables in the range of 20–650 °C was presented. The model results confirmed by experimental results. In the work presented by [22], a two-dimensional model of thermocline thermal storage system was designed to understand the effects of the properties of the storage media (both solid and liquid materials) and of the boundary conditions of the input flow on thermal performance of the storage system. The results show that the thermocline thickness increases by use of solar salts as heat transfer fluid and cofalit as a solid material.

[23] set up 30 kWh single-tank single-media thermal storage system to examine experimentally the thermocline formation and propagation during charge cycle for different flow rates. It was shown that increase in the flow rate and lower diffusion rate reduce the thermocline thickness. Thermo-physical properties of three different filler materials were investigated at 200 MWh pre-industrial thermal storage system by [24] and magnetite, basic oxygen furnace-slag, and river rock reported as promising candidates as filler materials for efficient thermal storage. [25] employed different rocks to study their applicability to a thermal storage system with temperature range between 250 and 350 °C. It was concluded that cipolin and quartzite are the good candidates to be used as filler materials if there is a direct contact with thermal oil. [26] performed an experimental study to compare the experimental results with analytical approach solutions derived from the one-dimensional two-phase without heat loss model and one-dimensional one-phase with heat loss model in the single-tank thermocline system. It was found that local thermal equilibrium assumption is inappropriate in the thermocline tank because the internal heat transfer in fluid and solid is dominant.

In this study, single-tank thermocline thermal energy storage discharge cycle analysis with computational fluid dynamics (CFD) was considered in order to investigate the streamlines and velocity and temperature distribution in the thermocline tank together with the effects of porosity, sphericity, and type of fluid on discharge efficiency and to suggest geometrical improvements for better tank efficiency.

Seven different heat transfer fluids having various specific heat capacity values were considered. In order to see the effect of porosity, three porosity values of 0.2, 0.3, and 0.4 were selected. The effect of the filler material geometry was included by using four different sphericity values of 0.33, 0.6, 0.7, and 1.0.

2 Mathematical Modeling

Since this study includes numerical investigation of the heat transfer, the flow pattern, and the total thermal energy (time dependent) of a thermal storage in a cylindrical tank, the mathematical model includes porous region parameters. To obtain the results, the governing equations of continuity, time-dependent momentum, and time-dependent energy must be solved. Governing equations include not only effective conductivity and Forchheimer–Brinkman approximation but also Boussinesq approximation. As validated by [27], the temperature difference between the solid and liquid in the porous region is ignored according to local thermal equilibrium model. The non-dimensional variables used are defined as in Eqs. 1, 2, 3.

$$X = \frac{x}{d_p}, Y = \frac{y}{d_p}, U = \frac{u}{U_0}, V = \frac{v}{U_0}, \theta = \frac{T - T_c}{T_h - T_c}, P = \frac{p}{\rho U_0^2} \tag{1}$$

$$k_{eff} = \xi k_f + (1 - \xi) k_p, \quad R_c = \frac{k_{eff}}{k_f} \tag{2}$$

$$\mathrm{Re} = \frac{U_0 L}{\upsilon}, Gr = \frac{g\beta(T_h - T_c)L^3}{\upsilon^2}, \mathrm{Pr} = \frac{\upsilon}{\alpha_f}, Da = \frac{K}{L^2} \tag{3}$$

Taking into account above-mentioned assumptions and dimensionless variables, the governing equations in the normalized state to represent the flow phenomenon in the clear liquid region are given in Eqs. 4, 5, 6, 7.

$$\frac{\partial U}{\partial X} + \frac{\partial V}{\partial Y} = 0 \tag{4}$$

$$U\frac{\partial U}{\partial X} + V\frac{\partial U}{\partial Y} = -\frac{\partial P}{\partial X} + \frac{1}{Re\left(\frac{\partial^2 U}{\partial X^2} + \frac{\partial^2 U}{\partial Y^2}\right)} \tag{5}$$

$$U\frac{\partial U}{\partial X} + V\frac{\partial U}{\partial Y} = -\frac{\partial P}{\partial X} + \frac{1}{\mathrm{Re}\left(\frac{\partial^2 V}{\partial X^2} + \frac{\partial^2 V}{\partial Y^2}\right)\frac{\mathrm{Gr}}{\mathrm{Re}^2}} \tag{6}$$

$$U\frac{\partial \theta}{\partial X} + V\frac{\partial \theta}{\partial Y} = \frac{1}{\mathrm{PrRe}\left(\frac{\partial^2 \theta}{\partial X^2} + \frac{\partial^2 \theta}{\partial Y^2}\right)} \tag{7}$$

At the same time, the general form of the governing equation in a porous region is based on the mean Navier–Stokes equations on the representative initial volume and is presented using the Darcy–Forchheimer–Brinkman model [27] and given in Eqs. 8, 9, 10, 11.

$$\frac{\partial U}{\partial X} + \frac{\partial V}{\partial Y} = 0 \tag{8}$$

$$\frac{1}{\xi^2}\left(U\frac{\partial U}{\partial X} + V\frac{\partial U}{\partial Y}\right) = -\frac{\partial P}{\partial X} + \frac{1}{\xi \mathrm{Re}\left(\frac{\partial^2 U}{\partial X^2} + \frac{\partial^2 U}{\partial Y^2}\right)\frac{1}{\mathrm{Re\,D\,a}}} \tag{9}$$

$$\frac{1}{\xi^2}\left(U\frac{\partial V}{\partial X} + V\frac{\partial V}{\partial Y}\right) = -\frac{\partial P}{\partial X} + \frac{1}{\xi \mathrm{Re}\left(\frac{\partial^2 V}{\partial X^2} + \frac{\partial^2 V}{\partial Y^2}\right)\frac{Gr}{\mathrm{Re}^2}\frac{1}{\mathrm{Re\,D\,a}}\frac{F}{\sqrt{\mathrm{Da}}}\sqrt{U^2 + V^2}} \tag{10}$$

$$U\frac{\partial \theta}{\partial X} + V\frac{\partial \theta}{\partial Y} = \frac{R_c}{\mathrm{Pr\ Re}\left(\frac{\partial^2 \theta}{\partial X^2} + \frac{\partial^2 \theta}{\partial Y^2}\right)} \tag{11}$$

Here, F is the inertia Forchheimer coefficient which can be mathematically expressed as in Eq. 12 [28].

$$F = \frac{1.75}{\sqrt{150\xi^3}} \tag{12}$$

where ξ is porosity and defined as fraction of void volume to total volume. The system permeability which depends on porosity, particle diameter, and particle sphericity is a measure of fluid transmission in porous medium. The permeability formula known as the Carmen–Kozeny Equation is presented in Eq. 13 [29].

$$K = \frac{\xi R^2}{8\tau} \tag{13}$$

3 Computational Fluid Dynamics Studies

Open source software openFOAM was used to perform CFD analysis of the thermocline storage tank. In order to perform simulations, governing equations described in the previous section has to be solved with appropriate boundary conditions. Therefore, governing equations were constructed based on PIMLPE. To interpret the control terms in the governing equations, the predicted scheme was used together with second-order planning which interprets the terms. In order to obtain converged solution, the optimal value of the relaxation factor was chosen based on computational experiments. The convergence criterion was set for relative residue of all variables and all components of speed and temperature as 10^{-6}.

Table 1 Average temperature at the middle of tank for different meshes

Mesh Size	100[a]-30[b]	100[a]-60[b]	200[a]-30[b]	200[a]-60[b]	400[a]-30[b]	400[a]-60[b]
Average temperature at the middle of tank, (K)	583.42	583.55	583.06	583.11	582.97	582.95

[a]number of vertical nodes, [b]number of horizontal nodes

3.1 Validation of the CFD Model

It is important to perform model validation before investigating the effect of various parameters on the tank performance. Therefore, a thermocline tank employed for experiments by [30] was used. Since, the inlet of tank is located at bottom, whereas the outlet is located at top of the tank, during discharging, cold fluid enters the tank from the bottom and hot fluid exits the tank from the top. Since tank design has symmetry around the cylindrical axis, two-dimensional simulations were considered. The corresponding boundary conditions in dimensionless form are given below.

- The tank has just one inlet and one outlet.
- Inlet and outlet flows are calculated based on Re number.
- Inlet flow temperature considered to be constant at low temperature.
- Tank walls have zero gradient boundary condition (heat losses are zero).
- At the interface of two fluid and porous medium zones, the following boundary conditions are applied:
- Effective viscosity equals to fluid viscosity $\mu_{eff} = \mu_f$ [27].
- Porous section has same temperature as fluid section due to small Re number.

The required simulation parameters were collected form [7] and [9].

For every CFD simulation, it is important to ensure grid independence of the results. Therefore, prior to comprehensive simulations, mesh sensitivity analysis was performed by generating six non-uniform meshes. Table 1 shows the variation of simulated average temperature in the middle of the tank for different meshes. It is seen that the difference between the results of the mesh having 3000 and 24,000 nodes is less than 0.1%. Considering the difference between the results and computational time, the simulations continued with 100 vertical-60 horizontal totaling 6000 nodes mesh configuration.

To validate the numerical model generated, the discharge process was simulated with the selected mesh and with similar time scale as experiments. Figure 1 shows that the numerical model used in this study shows good agreement with experimental data of [30].

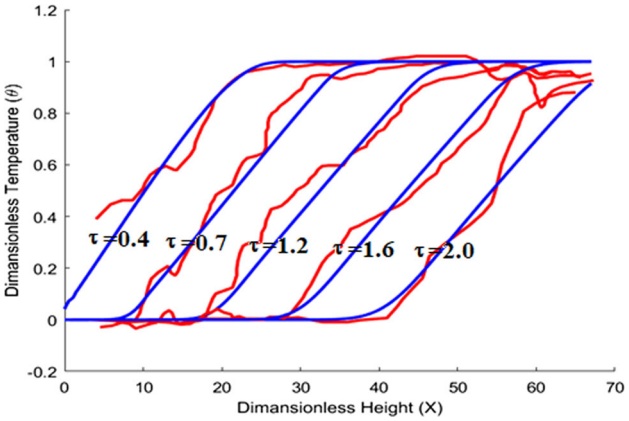

Fig. 1 Variation of dimensionless temperature with dimensionless height during discharge process (red: experiment, blue: simulation)

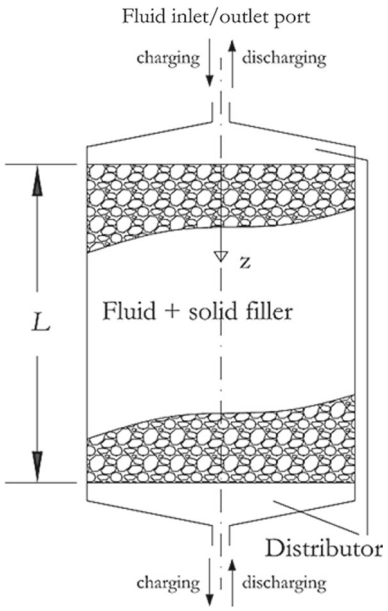

Fig. 2 Tank geometry used in this study [7]

4 Results

The tank geometry adopted is from [7] at which the sensitivity analysis of tank height, solid thermo-physical properties, and fluid properties were performed (Fig. 2).

The solid filler used in this study is 0.1 m diameter quartzite having density of 2500 kg/m^3 and specific heat value of 830 J/kg-K making its volumetric heat capacity 2.08 MJ/m^3-K. The fluids considered are shown in Table

Table 2 Properties of heat transfer fluids considered in this study

Heat Transfer Fluid	Density (kg/m^3)	Specific Heat (J/kg-K)	Volumetric Heat Capacity (MJ/m^3-K)	Thermal Conductivity (W/m-K)	Working Temperature (°C)
Pressurized Air (20 bar, 600 K)	11.6	1056	0.01	0.046	<1000
Supercritical CO_2 (80 bar, 600 K)	72	1140	0.08	0.04	<850
Sodium (liquid)	820	1290	1.06	60	285–873
Lead–Bismuth Eutectic	9500	120	1.14	15	285–1650
Synthetic Oils	850	2200	1.87	1	<400
Solar Salt	1790	1500	2.69	0.5	290–590
HITEC Salt	1870	1561	2.92	0.2	<538

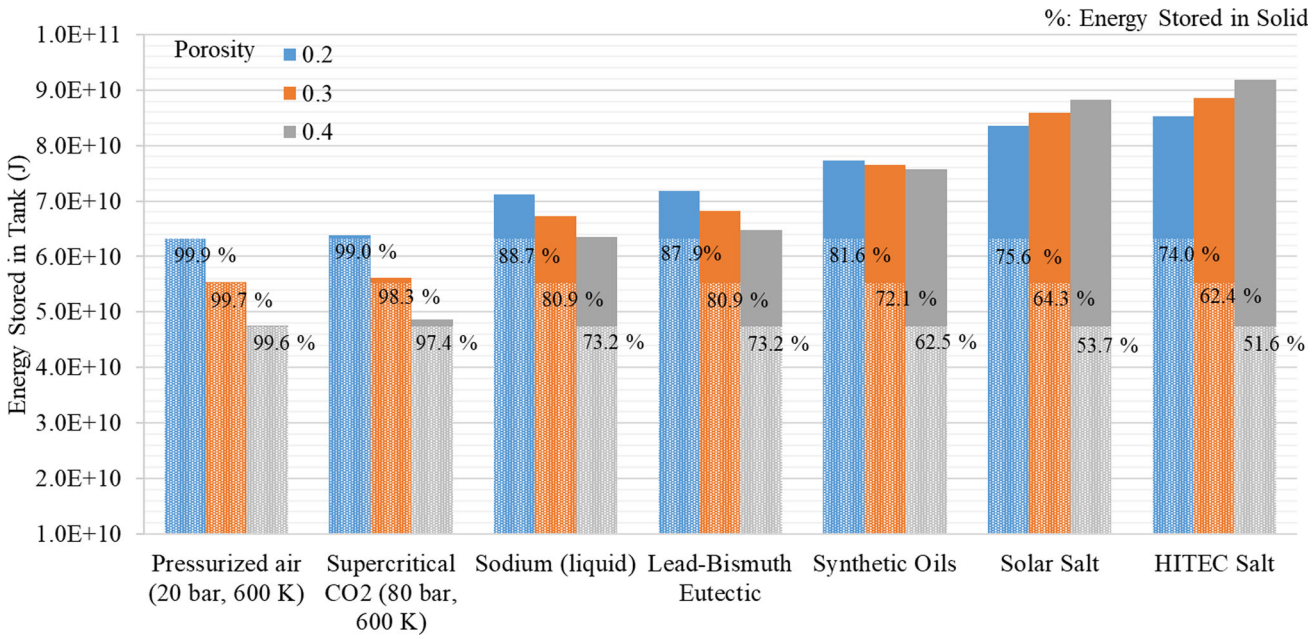

Fig. 3 Total energy stored in the tank before discharge and the percentage of that energy stored in solid filler material (dotted parts)

2. The fluids are selected according to working temperature of the proposed system which is between 554 and 664 K.

In energy storage problems, the volumetric heat capacity defines how much energy can be carried with the fluid from solar field to storage tank as well as percentage of energy stored in fluid and solid at every stage of the charge/discharge cycle. For the same operating conditions, i.e., type and amount of solid filler, porosity, and temperature, each fluid results in different initial stored energy in the tank as seen in Fig. 3. Although it is not the commercial practice to use different fluids at the same thermal conditions due to the fact that each fluid has an operating temperature which provides the maximum efficiency to system, the same thermal conditions and the same velocity at inlet and outlet of the tank were assumed in this study to compare the effect of other parameters. It is clear from Fig. 3 that for the same porosity value, as volumetric heat capacity value of the fluid increases, total energy stored in the system increases since more energy is carried by the fluid from heat exchanger.

In addition, as porosity increases, total energy stored in the tank decreases except for cases when Solar Salt and HITEC Salt used as working fluid. The reason of this trend is due to the fact that the increase in porosity results in more fluid in the tank therefore reduces the total energy stored in the tank for systems where solid volumetric heat capacity value is higher than fluid volumetric heat capacity value. On the other hand, if solid filler material has volumetric heat capacity value less than the fluid, then the amount of energy stored in the tank increases with porosity.

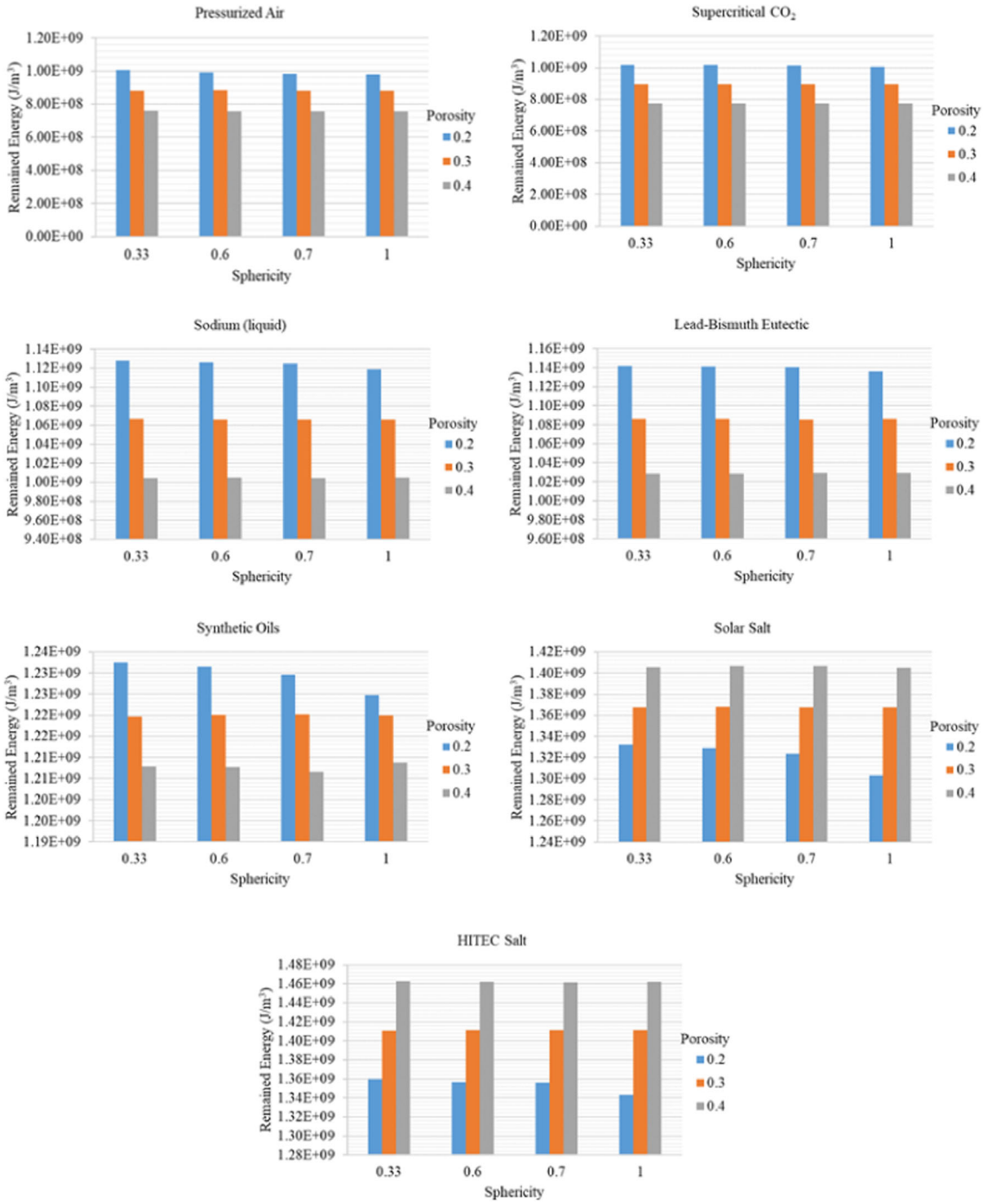

Fig. 4 The energy remained in tank after 3 h of discharge

The percentage of total initial energy stored in solid is also given in Fig. 3 (dotted areas). It is clear that for the same porosity value, when the fluid volumetric heat capacity value decreases, more energy is stored in the solid filler material. This is the desired operation since solid filler material is considered as the main storage component of the system. In addition, when porosity increases, energy stored in solid decreases due to the fact that amount of fluid in the tank increases with high value of porosity. This decrease is more significant when solid and fluid materials have comparable volumetric heat capacity values.

In order to analyze discharge process, first 3 h of discharge was simulated. The energy remained in the tank after 3 h of discharge for all fluids is given in Fig. 4. It is clear from Fig. 4 that as fluid volumetric heat capacity increases, the energy remained in the tank increases. This increase is

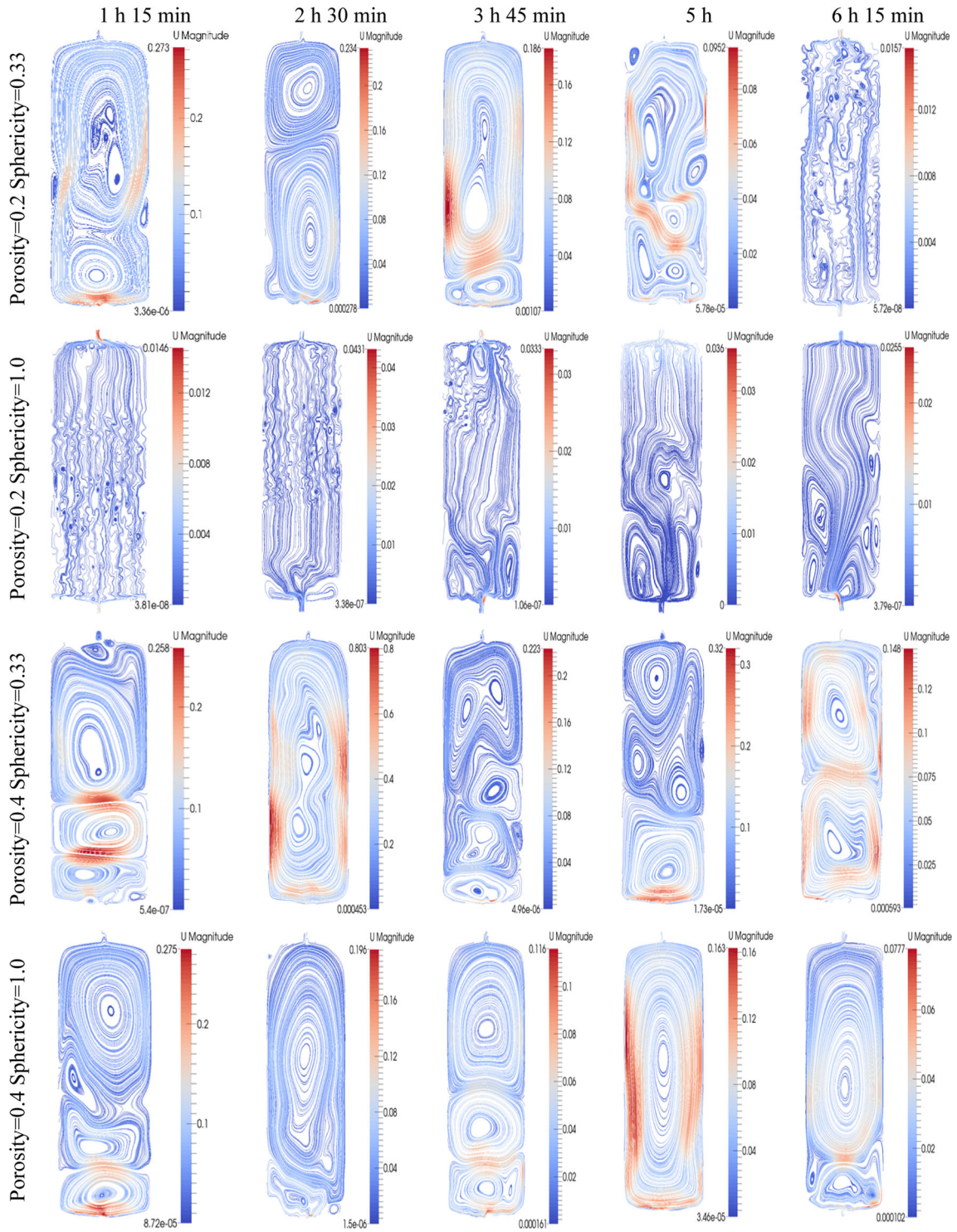

Fig. 5 Variation of streamline of Pressurized Air during 6 h of discharge

more pronounced for fluids having volumetric heat capacity values greater than the solid filler material. The trend does not change with different porosity or sphericity values. On the other hand, increase in porosity decreases the amount of energy remained in the tank for all cases except for the cases where Solar Salt and HTEC Salt used as working fluid. It should be noted that when solid has volumetric heat capacity value higher than the fluid's, it acts as the main storage component of the system. During the discharge cycle, solid filler transfers the energy to cold fluid efficiently and energy

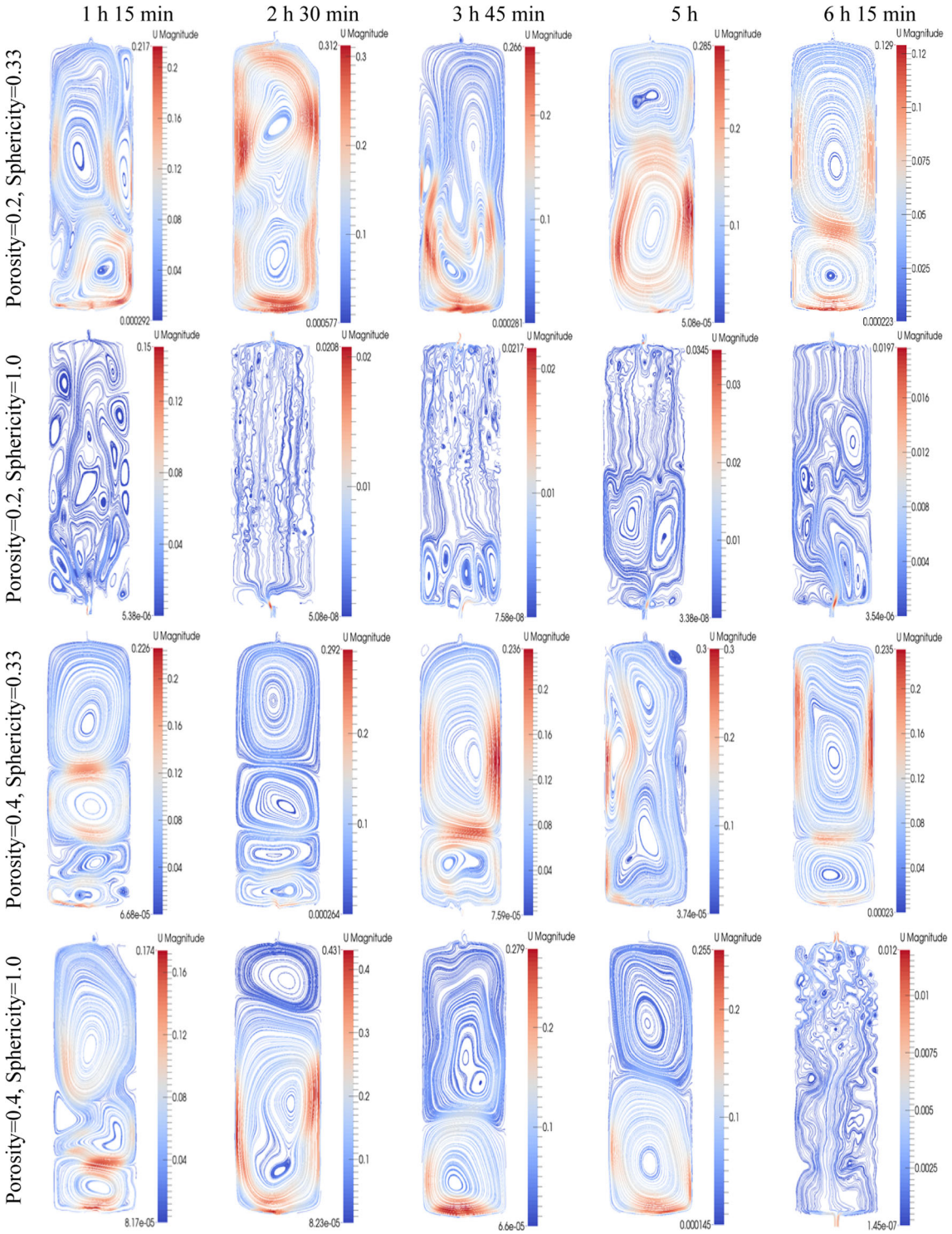

Fig. 6 Variation of streamline of Solar Salt during 6 h of discharge

remained in the tank decreases. On the other hand, when fluid acts as main storage component of the system which is when fluid has higher value of volumetric heat capacity than solid filler material, cold fluid does not receive enough energy from solid. The effect of sphericity on the discharge process can only be seen when the porosity value reaches 0.2. For this case, increase in sphericity results in decrease in energy remained in the tank.

The calculation of energy remained in the tank alone is not a clear indication of the tank performance since when

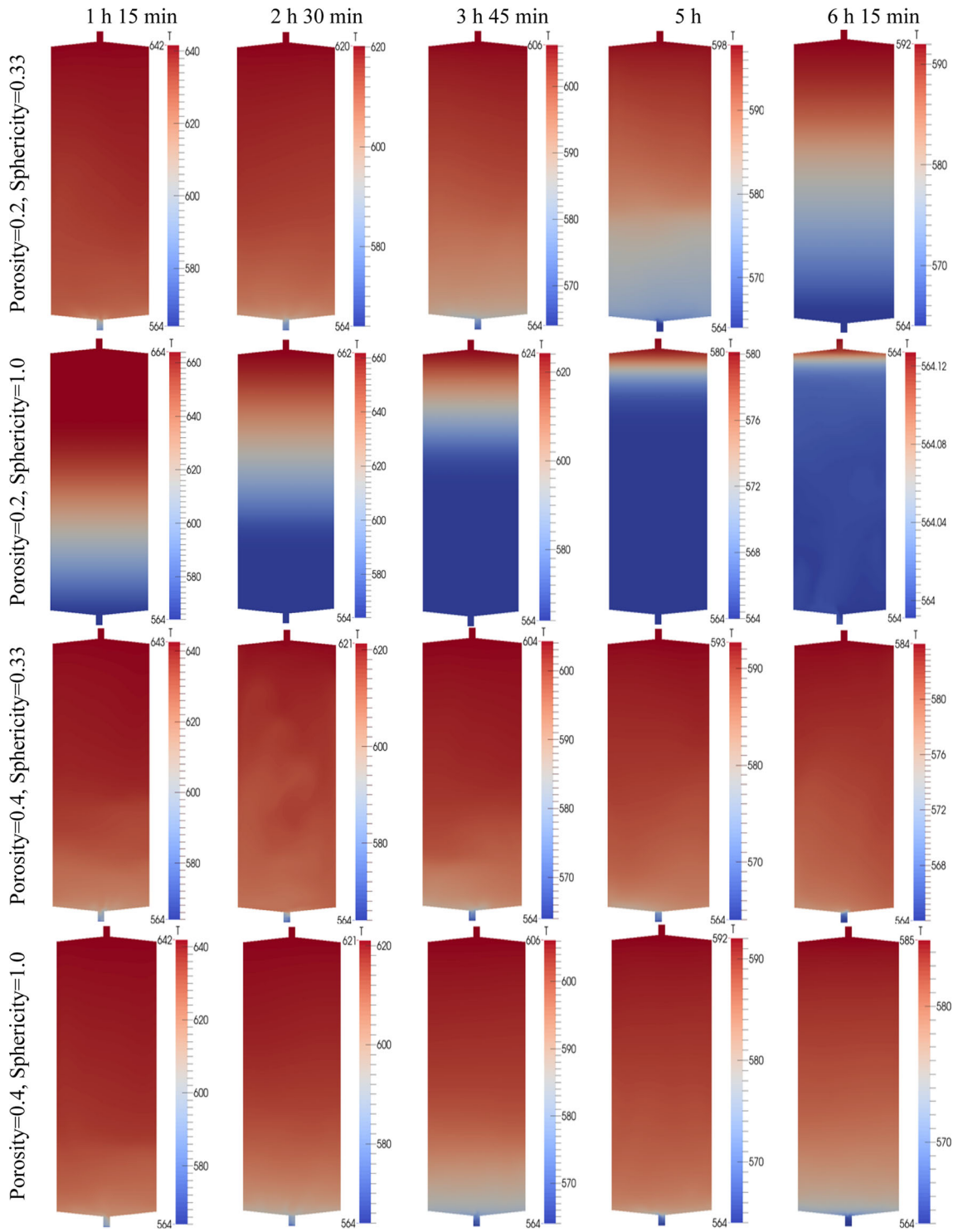

Fig. 7 Variation of temperature of Pressurized Air during 6 h of discharge

clod and hot fluids are mixed, power capacity of the tank decreases. Rather, streamline and temperature distribution analysis provides good opportunity to understand behavior of the tank with time. Since it was shown before that tank behavior is mainly affected by the rate of volumetric heat capacity of fluid and solid filler material, two fluids having minimum (Pressurized Air) and maximum (Solar Salt) volumetric heat capacity values in Table 2 were selected for streamline and temperature distribution presentation. In addition, minimum and maximum sphericity (0.33 and 1.0) and porosity (0.2 and

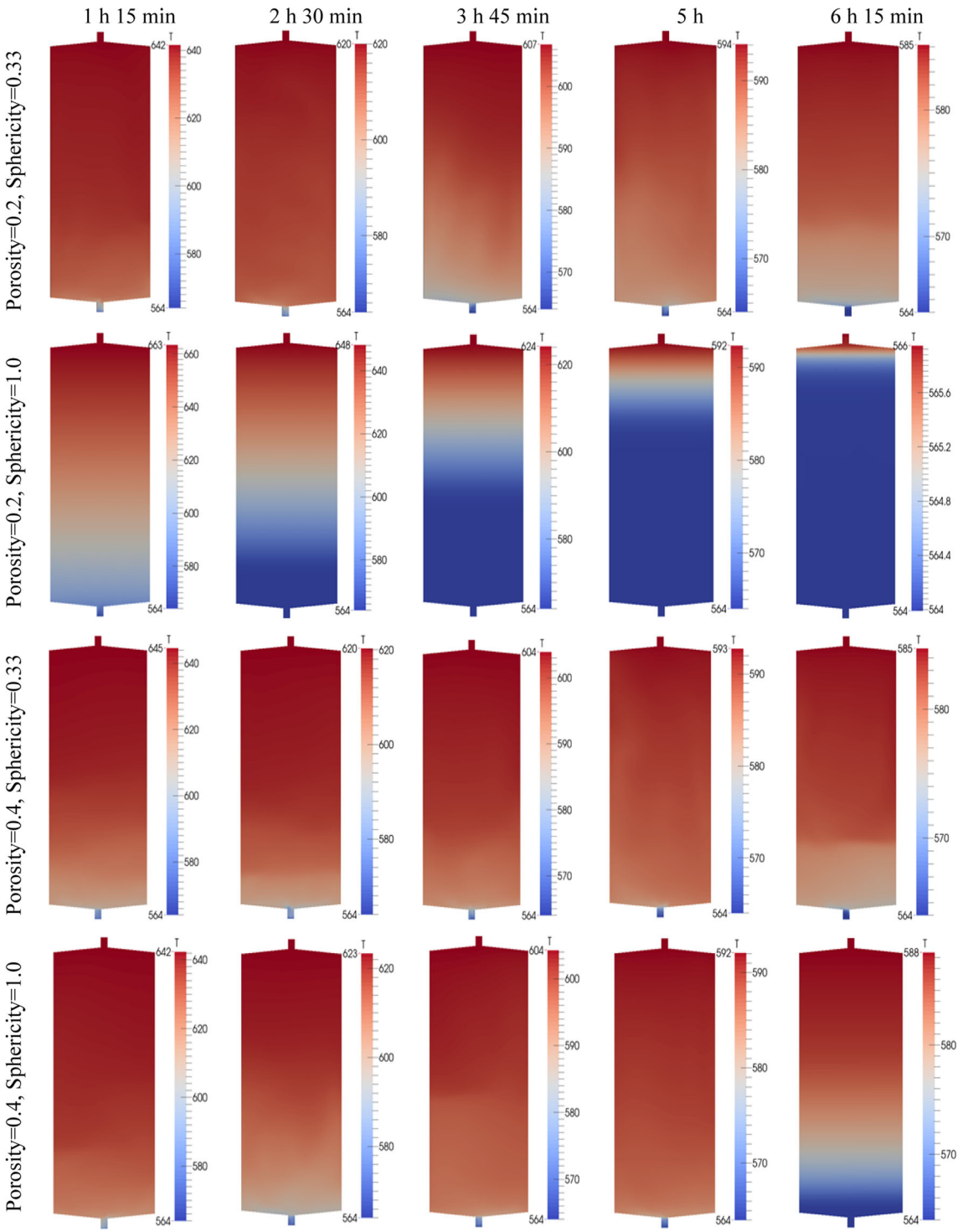

Fig. 8 Variation of temperature profile of Solar Salt during 6 h of discharge

0.4) values were selected for inter comparison. The simulations were performed for 6 h of discharge.

During discharge, streamlines are preferred to be either uniform or close to uniform to prevent mixing of hot and cold fluids. In this study, it was found that streamlines are much more uniform for both Pressurized Air and Solar Salt when porosity equals to 0.2 which is the minimum value and when sphericity equals to 1 which is the maximum value (Figs. 5, 6). This indicates less mixing in the tank. The timeline of the discharge cycle shown in Fig. 7 and Fig. 8 supports this

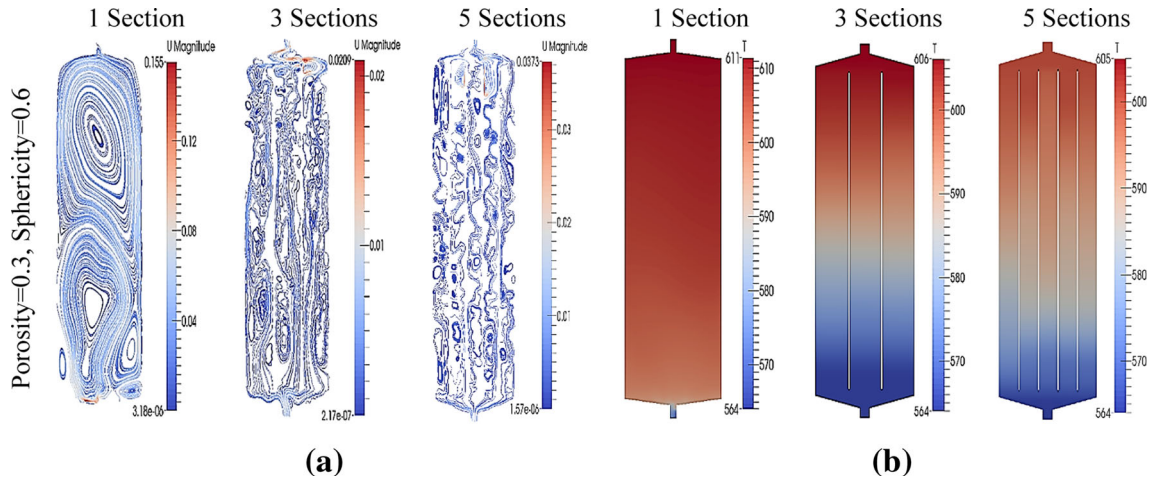

Fig. 9 Streamlines (**a**) and temperature profiles (**b**) for Pressurized Air after 3 h of discharge

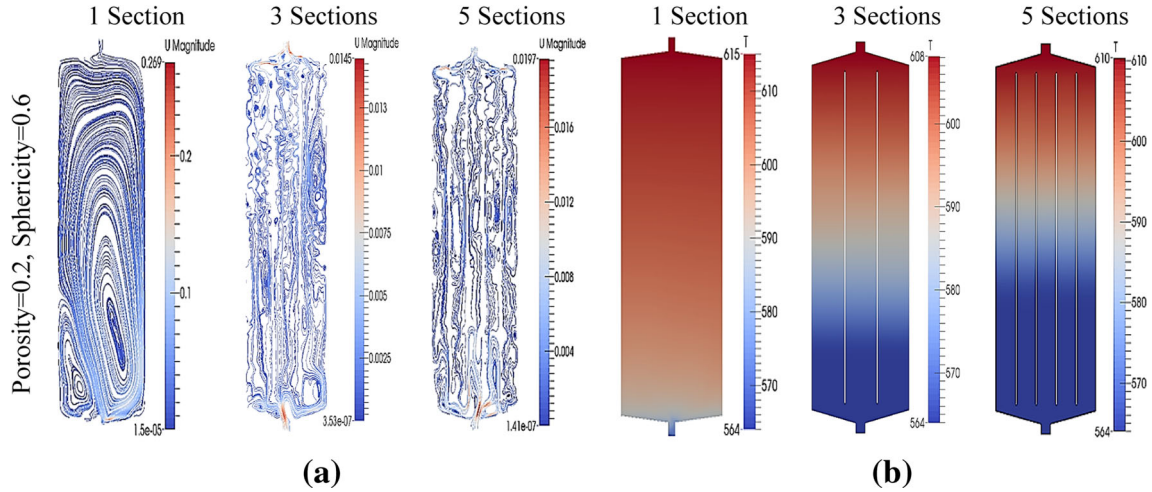

Fig. 10 Streamlines (**a**) and temperature profiles (**b**) for Solar Salt after 3 h of discharge

outcome since low porosity and high sphericity case results in faster discharge and less mixing. The thermocline movement can clearly be seen from temperature profiles in Fig. 6 and Fig. 8 that cold fluid moves from the bottom of the tank toward to top and there is a clear distinction between the cold and hot fluids. In addition, regardless of the sphericity value, high porosity in the tank causes mixing in the tank therefore deteriorates the tank performance.

It is clear from Fig. 9 and 10 that additional walls inside the tank reduced severity of vortexes and improved streamlines by making them more uniform. Although uniform streamlines are good indicators of improvement of the tank performance, it is good to look for power produced by the tank. Table 3 shows the percent increase at the tank power with above-mentioned geometrical modifications. As a result of comparison with the original design, it was concluded that sectioning of the tank volume improves the tank performance around 30% for both fluids. It can also be concluded from Table 3 that further sectioning will not improve tank performance in great amount because the values of 3 sections and 5 sections are very close to each other. In addition, the installation of the walls inside the tank diminished the effect of porosity, sphericity, and fluid type on tank thermal performance.

5 Conclusions

In this work, the aim was to investigate the effect of various parameters on single-tank thermocline energy storage system discharge performance to provide insight to selection process of operational parameters and materials for the system. In addition, thermal performance improvements were investigated. The simulations were performed with computational fluid dynamics techniques to fully integrate the mathematical models into calculations without any simplification. Seven

Table 3 Comparison of power generated by the single section tank with the tanks with three and five sections

Fluid	Modification	Porosity	Sphericity			
			0.33	0.6	0.7	1.0
Pressurized Air (20 bar, 600 K)	3 sections	0.2	29.88	24.05	26.39	30.65
		0.3	28.15	33.56	32.58	32.82
		0.4	31.33	28.95	29.28	29.66
	5 sections	0.2	32.19	33.22	30.56	32.04
		0.3	28.46	32.65	31.74	35.34
		0.4	31.90	31.43	30.58	31.73
Solar Salt	3 sections	0.2	30.84	33.48	31.34	28.47
		0.3	28.36	29.18	29.52	30.82
		0.4	29.56	29.57	30.74	29.19
	5 sections	0.2	32.86	39.18	36.71	29.81
		0.3	29.83	30.90	31.41	29.54
		0.4	30.05	31.22	32.43	30.70

different working fluids, three different porosity values, and finally four different sphericity values were considered for parametric study. Energy stored, temperature profiles, and streamlines in the tank after 3 or 6 h of discharge process were presented.

The simulation results indicated that the most important parameter for the storage system is the ratio of volumetric heat capacity value of the working fluid and solid filler material. This ratio changes the behavior of the tank completely. The percentage of the stored energy in the solid drops as low as 50% if the fluid has high volumetric heat capacity and tank has high porosity. The effect of sphericity on the tank performance is not significant for high values of porosity. For the smallest value of porosity considered in this study, an increase in sphericity resulted in decrease in amount of remaining energy in the tank. On the other hand, temperature profiles and streamlines of the 6 h of discharge showed that for low values of porosity, higher sphericity value prevents mixing of hot and cold fluid and results in better discharge performance.

The investigation of streamlines showed that eddies and vortexes get larger and divide the tank into two or more regions. Since these regions are not connected to each other as convection type, the heat transfer between them occurs just as conduction type. As a result, heat transfer performance deteriorates. In order to overcome this issue, the tank interior was divided into three and five section with walls. The streamlines showed that mixing is reduced and flow is more uniform and tank performance is improved. The tank power increases around 30% due to sectioning performed inside the tank.

Future studies can be done to increase the efficiency of the tank by improving streamline pattern. It is possible to reach this goal by making modifications inside the tank such as creating lanes for the flow. Another possible area of study can be usage of nano-fluids as heat transfer medium. These studies can be performed efficiently with computational fluid dynamics simulations which use the experimentally verified mathematical model developed in this study.

References

1. Brenna, M.; Foiadelli. F.; Roscia, M.; Zaninelli, D.: Evaluation of solar collector plant to contribute climate change mitigation, Proceedings of the IEEE international conference sustainable energy technology, ICSET, (2008)
2. Khan, J.; Arsalan, M.H.: Solar power technologies for sustainable electricity generation – a review. Renew. Sustain. Energy Rev. **55**, 414–425 (2016)
3. Reddy, S.V.; Kaushik, S.C.; Tyagi, S.K.: Year round performance and economic evaluation of solar power plant for Indian tropical condition. J. Renew. Sustain. Energy **4**, 4–13 (2012)
4. Kaushika, N.D.; Reddy, K.S.: Performance of a low cost solar paraboloid dish steam generating system. Energy Conversat. Manag. **41**, 713–726 (2000)
5. Gil, A.; Medrano, M.; Martorell, I.; Lazaro, A.; Dolado, P.; Zalba, B.; Cabeza, L.: State of the art on high temperature thermal energy storage for power generation. Renew. Sustain. Energy Rev. **14**, 31–55 (2010)
6. Brosseau, D.; Hlava. P.; Kelly, M.: Testing thermocline filler materials and molten-salt heat transfer fluids for thermal energy storage systems used in parabolic trough solar power plants. Sandia national laboratories, Albuquerque NM, Technical report, 3207, (2004)
7. Bonanos, A.M.; Votyakov, E.V.: Sensitivity analysis for thermocline thermal storage tank design. Int. J. Heat Mass Transf. **37**, 939–954 (2016)
8. Fernández-Torrijos, M.; Sobrino, C.; Almendros-Ibáñez, J.A.: Simplified model of a dual-media molten-salt thermocline tank with a multiple layer wall. Sol. Energy **151**, 146–161 (2017)
9. Yang, Z.; Garimella, S.: Thermal analysis of solar thermal energy storage in a molten-salt thermocline. Sol. Energy **84**, 974–985 (2010)
10. Yin, H.; Ding, J.; Jiang, R.; Yang, X.: Thermocline characteristics of molten-salt thermal energy storage in porous packed-bed tank. Appl. Therm. Eng. **110**, 855–863 (2017)

11. Xu, C.; Wang, Z.; He, Y.; Li, X.; Bai, F.: Sensitivity analysis of the numerical study on the thermal performance of a packed-bed molten salt thermocline thermal storage system. Appl. Energy **92**, 65–75 (2012)
12. Bayon, R.; Rojas, E.: Simulation of thermocline storage for solar thermal power plants: from dimensionless results to prototypes and real-size tanks. Int. J. Heat Mass Transf. **60**, 713–721 (2013)
13. Flueckiger, S.; Yang, Z.: Review of molten-salt thermocline tank modeling for solar thermal energy storage. Heat Mass Transf. Eng. **34**, 787–800 (2013)
14. Li, P.; Lew, J.V.; Karaki, W.; Chan, C.; Stephens, J.; Wang, Q.: Generalized charts of energy storage effectiveness for thermocline heat storage tank design and calibration. Sol. Energy **85**, 2130–2143 (2011)
15. Votyakov, E.; Bonanos, A.: A perturbation model for stratified thermal energy storage tanks. Int. J. Heat Mass Transf. **75**, 218–223 (2014)
16. Meng-Jie, Li.; Qiu, Y.; Ming-Jia, Li.: Cyclic Thermal performance analysis of a traditional single-layered and of a novel multi-layered packed-bed molten salt thermocline tank. Renew. Energy **118**, 565–578 (2018)
17. ELSihy, E.S.; Xu, C.; Du, X.: Cyclic performance of cascaded latent heat thermocline energy storage systems for high-temperature applications. Energy (2021). https://doi.org/10.1016/j.energy.2021.122229
18. Vannerem, S.; Neveu, P.; Falcoz, Q.: Experimental and numerical investigation of the impact of operating conditions on thermocline storage performance. Renew. Energy **168**, 234–246 (2021)
19. Reddy, K.S.; Pradeep, N.: Stability analysis of the thermocline thermal energy storage system during high flow rates for solar process heating applications. Sol. Energy **226**, 40–53 (2021)
20. Brown, N.; Lai, F.: Enhanced thermal stratification in a liquid storage tank with a porous manifold. Sol. Energy **85**, 1409–1417 (2011)
21. Forsberg, C.; Peterson, P.; Zhao, H.: High-temperature liquid-fluoride-salt closed-brayton-cycle solar power towers. J. Sol.Energy Eng. **129**, 141–146 (2007)
22. Chang, Z.; Li, X.; Xu, C.; Chang, C.; Wang, Z.: The design and numerical study of a 2 MWh molten salt thermocline tank. Proceedings of Solar PACES, (2014)
23. Gajbhiye, P.; Salunkhe, N.; Kedare, S.; Bose, M.: Experimental investigation of single media thermocline storage with eccentrically mounted vertical porous flow distributor. Sol. Energy **162**, 28–35 (2018)
24. Grosu, Y.; Ortega-Fernández, I.; González-Fernández, L.; Udayashankar, N.; Filali Baba, Y.; Al Mers, A.; Faik, A.: Natural and by-product materials for thermocline based thermal energy storage system at CSP plant: structural and thermophysical properties. Appl. Therm. Eng. **136**, 185–193 (2018)
25. Grirate, H.; Agalit, H.; Zari, N.; Elmchaouri, A.; Molina, S.; Couturier, R.: Experimental and numerical investigation of potential filler materials for thermal oil thermocline storage. Sol. Energy **131**, 260–274 (2016)
26. Chang, Z.; Li, X.; Falcoz, Q.; Wang, Z.; Neveu, P.: Approximate analytical characterization and multi-parametric optimization design of single-tank thermocline heat storage system. Appl. Therm. Eng. **181**, 116010 (2020)
27. Taghizadeh, S.; Asaditaheri, A.: Heat transfer and entropy generation of laminar mixed convection in an inclined lid driven enclosure with a circular porous cylinder. International Journal of Thermal Science **134**, 242–257 (2018)
28. Alazmi, B.; Vafai, K.: Analysis of variants within the porous media transport models. J Heat Trans **122**, 303–326 (2000)
29. Antonio, C.: Permeability-porosity relationship: A reexamination of the Kozeny-Carman equation based on a fractal pore-space geometry assumption. Geophys. Res. Lett. **33**, 1–5 (2006)
30. Pacheco, J.; Showalter, S.; Kolb, W.: Development of a molten-salt thermocline thermal storage system for parabolic trough plants. Sol. Energy **124**, 153–159 (2001)